BMC Oral Health

Research article

Laser-induced breakdown spectroscopy: a tool for real-time, *in vitro* and *in vivo* identification of carious teeth

Ota Samek*[1], Helmut H Telle[2] and David CS Beddows[3]

Address: [1]Institute of Physical Engineering, Technical University Brno, Technická 2, 616 69 Brno, Czech Republic, [2]Department of Physics, University of Wales Swansea, Singleton Park, Swansea SA2 8PP, United Kingdom and [3]Department of Chemistry, The University of Edinburgh, West Main Roads, Edinburgh EH9 3JJ, United Kingdom

E-mail: Ota Samek* - samek@ufi.fme.vutbr.cz; Helmut H Telle - h.h.telle@swansea.ac.uk; David CS Beddows - pybeds@hotmail.com

*Corresponding author

Published: 19 December 2001

BMC Oral Health 2001, **1**:1

Received: 17 October 2001

Accepted: 19 December 2001

This article is available from: http://www.biomedcentral.com/1472-6831/1/1

Abstract

Background: Laser Induced Breakdown Spectroscopy (LIBS) can be used to measure trace element concentrations in solids, liquids and gases, with spatial resolution and absolute quantifaction being feasible, down to parts-per-million concentration levels. Some applications of LIBS do not necessarily require exact, quantitative measurements. These include applications in dentistry, which are of a more "identify-and-sort" nature – e.g. identification of teeth affected by caries.

Methods: A one-fibre light delivery / collection assembly for LIBS analysis was used, which in principle lends itself for routine *in vitro* / *in vivo* applications in a dental practice. A number of evaluation algorithms for LIBS data can be used to assess the similarity of a spectrum, measured at specific sample locations, with a training set of reference spectra. Here, the description has been restricted to one pattern recognition algorithm, namely the so-called Mahalanobis Distance method.

Results: The plasma created when the laser pulse ablates the sample (*in vitro* / *in vivo*), was spectrally analysed. We demonstrated that, using the Mahalanobis Distance pattern recognition algorithm, we could unambiguously determine the identity of an "unknown" tooth sample in real time. Based on single spectra obtained from the sample, the transition from caries-affected to healthy tooth material could be distinguished, with high spatial resolution.

Conclusions: The combination of LIBS and pattern recognition algorithms provides a potentially useful tool for dentists for fast material identification problems, such as for example the precise control of the laser drilling / cleaning process.

Background

Numerous techniques have been devised to examine dental caries; many of these have been reviewed e.g. by Murray [1] and Niemz [2]. However, most promising some newly emerging technological realisations in analytical spectroscopy, including laser fluorescence (already a commercial diagnostic system *KaVo DIAGNOdent* is available) [3,4], digital imaging fibre optics transillumination [4,5], tuned-aperture computer tomography [6,7], and digital radiography [6,8]. The great sensitivity of some of these

methods allows the detection of caries at earlier stage than conventional methods [1,2,9]. Unfortunately, none of these techniques can normally be used for real-time detection of demineralized enamel / dentin (accompanied with loss of calcium *Ca* and phosphorus *P*[10]), associated with caries, directly during the application of laser drilling.

In recent years research groups particularly in Germany have shown that the use of femto-second lasers may present an alternative to classical mechanical drilling techniques to realise contactless drills in dentistry [2,11,12]. While intriguingly elegant, femto-second laser drilling still experiences problems with ablation efficiency [11,12]. For example, some dentists utilise Er:YAG lasers [12,13], which were recently approved by the US Food and Drug Administration (FDA) for use on human subjects [14]. Er:YAG lasers have greater efficiency than other, presently available femto-second laser systems. However, drill areas treated by Er:YAG lasers occasionally contain long fissures that arise due to sudden vaporisation of the water in the tooth tissue [11,12,15]. This may result in rough tooth surfaces with deep cracks, up to 300 μm; their presence and extent were detected using dye penetration tests [2]. Because of such cracks, acids can penetrate to the tooth and may be the source of new carious lesions. Although some authors reported that micro-cracks are avoidable [13,14,16], it is obvious that their appearance depends on the specific ablating conditions; presently a common consensus regarding the appearance of cracks does not seem to exist (see Eguro *et al*[17]). On the other hand, it has been reported that changing the laser wavelength from the IR/visible to the UV may largely overcome the problem of mechanical stress, which causes said problem [18]. Therefore, despite the current problems it is likely that in the near future, with further development of novel laser systems, the clinical application of femto-second pulsed laser drilling may emerge as a real alternative to mechanical / Er:YAG-laser dental treatment. Hence, regardless of the ultimately selected laser system, methods are required to monitor the drilling process.

Here we propose a method based on the technique of Laser Induced Breakdown Spectroscopy (LIBS), capable of monitoring the laser drilling process by monitoring and analysing the luminescent plasma – *in vivo* and in real time; thus precise control of ablated material can be achieved. In the dental practice, usually more healthy tissue than ultimately necessary is removed. The monitoring mainly depends on a "human" factor – the visual inspection by the dentist. The plasma, which is created during the ablation using short laser pulses, can be spectrally analysed using a one-fibre light delivery and collection system.

To use the spectroscopic analysis of laser-induced plasmas, to obtain information about the caries – state of dental tissue, was first suggested by Niemz [2] and Kohns [12]. Their studies involved only the spectroscopic investigation of spectral lines of calcium (intensity and line width). However, using just a few spectral lines of a single element is known to potentially be a source of large errors in any laser analytical technique like LIBS. To our knowledge, there has been no study, except by our group [21], to simultaneously exploit the spectral information from more than one element, from matrix and non-matrix elements, in distinguishing between healthy and carious tissue. This novel approach constitutes part of our present investigation. The distinction between healthy and carious tissue can be very sensitive when exploiting spectral data from a pair, or even more than one pair, of suitable elements in the form of line intensity ratios combined with a pattern recognition algorithm.

Carious / healthy tooth material can be identified through the decrease of matrix elements (*Ca* and *P*) and/or the increase of non-matrix elements (typically *Li*, *Sr*, *Ba*, *Na*, *Mg*, *Zn* and *C*), using pattern recognition algorithms. This analysis process can be carried out with spatial resolution. Lateral precision of order of 100–200 μm, while depth profiling is accurate to less than 10 μm. Thus, in principle, the combination of LIBS and a pattern recognition algorithm gives dentists a powerful tool for precise real-time monitoring and identification of caries-affected tissue or dental restorative materials in the course of laser drilling.

As a note of caution we like to stress right from the outset that the laser used in this study, namely a Nd:YAG laser operating at its fundamental wavelength and providing pulses of nanosecond duration, is most likely not the laser of choice for actual *in vivo* laser drilling of teeth. Furthermore, no full clinical tests have been carried out thus far, only a single *in vivo* measurement was performed on a tooth of a volunteer. Therefore, the results reported here should be seen as a proof of principle, rather than the provision of a fully-developed technique immediately applicable in the dental practice.

Method and materials

In laser-induced breakdown spectroscopy one utilises the high power densities obtained by focusing the radiation from a pulsed laser (normally operating at a single, fixed wavelength), to generate a luminous micro plasma from the analyte (solid, liquid and gaseous samples). To a good approximation, the plasma composition is representative of the analyte's elemental composition. In the thirty years or so since its inception the potential of LIBS as an analytical tool has been realised, leading to an ever increasing list of applications, both for analysis in the laboratory and industrial environments [19,20]. We would like to note

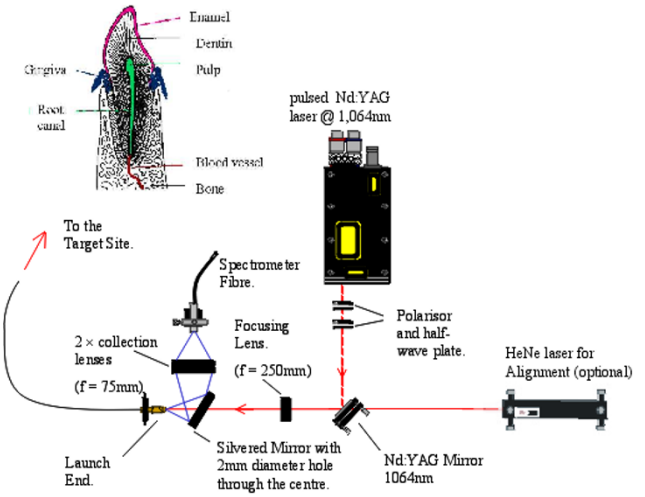

Figure 1
Plan view of the optical layout and the experimental equipment.

that the ablation of dental tissue using pulsed lasers, and simultaneously monitoring the plasma emission closely mimics the principle behind the technique of LIBS [21].

Standard LIBS analysis systems comprise typical major component units, namely (a) the laser source; (b) the laser light delivery and plasma emission collection system; and (c) the system for spectral analysis. For the experimental study described here, i.e. the implementation of LIBS in dentistry we used a fibre-based LIBS assembly [22].

The laser system

The laser used for plasma generation was a standard pulsed Nd:YAG laser (Quantel *Brilliant* or *BigSky*), operating at its fundamental wavelength of 1064 nm, at 20 Hz repetition rate. Individual laser pulses had a pulse length of 4–8 ns (depending on the Q-switch timing adjustment of the laser power supply). The pulse energy was precisely controlled using a half-wave retardation plate and Glan-laser polarizer in the beam path. It was measured using a calibrated energy meter (Coherent *LabMaster*); typically, pulse energies in the range 10–30 mJ were utilised. We would like to note here, that near IR lasers of nanosecond pulse duration most likely will not be the lasers of choice in practical applications for dental drilling, but should be viewed as a proof-of-principle scenario.

The light delivery and collection system

The overall optical arrangement used in our experiments is shown in Figure 1. A single fibre of core diameter 550 µm (Ensign-Bicford *HCG550*) and length 5 m was used to deliver the laser radiation to the target material (tooth) – for *in vivo* and *in vitro* applications -, and to collect the generated plasma emission for subsequent analysis. The fibre end-faces were prepared by a cleaving process which allowed irradiances of >1 GW/cm^2 to be transported without causing damage to the fibre.

As shown in the set-up, radiation from the Nd:YAG laser was focussed onto the launch end of the fibre, positioned just beyond the focal point of the lens, via a high reflectivity mirror (coated to R>99.5% at 1,064 nm) using a 250 mm focal length converging lens. This radiation was passed through a centre hole of 2 mm diameter in the light-collection mirror.

The laser light pulses exiting the far end of the fibre (distal-end) were directed onto the target material. Note that for a large fraction of our experiments no optical components were used between the fibre end and the tooth. The separation between the fibre and the target (tooth) was about $D \neq 1.5–2.0$ mm. Taking into account this fibre-to-target distance and the fibre's numerical aperture (NA = 0.22), the irradiance on target is of the order $I_T \neq 0.092–0.065$ GW/cm^2, for a launch pulse energy of E_{pf} = 12 mJ. This value is safely above the threshold for the generation of a luminous plasma, which we determined as about $I_{T,th} \neq 0.05$ GW/cm^2.

A fraction of the light emitted from the target surface was collected via the same fibre; this re-emerges at the launch end (proximal-end), with a divergence relating to the numerical aperture of the fibre. The mirror with an UV-enhanced metallic coating was used to separate this diverging light from the in-coming Nd:YAG laser pulses. This (diverging) plasma fluorescence light was re-focused onto the spectrograph fibre bundle. Note that the fibre assembly can be used to just collect the light from the plasma simply by placing the distal end close to the target, in case that the laser pulses are not delivered through the same optical fibre for the drilling of dental tissue.

For optional assistance in precise pointing of the near-IR ablation radiation onto particular areas of the tooth, light from a HeNe laser could be introduced collinearly via the Nd:YAG beam steering mirror (high transmission at 633 nm).

The system for spectral analysis

The system used for spectral analysis consisted of a standard spectrograph (ACR500, *Acton Research*) with a gateable, intensified photodiode array detector (IRY1024, *Princeton Instruments*) attached to it. The gating of the detector and the timing for spectral accumulation were controlled by a PC via a pulse delay generator (PG200, *Princeton Instruments*).

We would like to note that the experimental results presented here were obtained using laser pulses of a few nanosecond duration. Precise time gating of the system for plasma analysis is normally needed, to avoid the strong, broadband spectral contribution from *Bremsstrahlung* during the early phase of the plasma evolution [23] (largely due to plasma – laser radiation interaction). Exploiting the pattern recognition algorithm, described later in this paper, the time-gating of the detection system does not have to be overly critical: unwanted broadband background contributions are automatically accounted for. Thus the acquisition time can be set as high as a few milliseconds [24], rather than the usual microsecond intervals; only proper synchronisation to the laser pulse is required, in principle. Hence, less sophisticated delay generators / electronics and photon detectors, such as e.g. simple photomultiplier tubes / high-gain avalanche diodes could suffice in the construction of a cost-effective device to monitor light from the luminous plasma. Furthermore, we like to note that for laser pulses of picosecond or sub-picosecond duration the plasma – laser radiation interaction is much shorter, and normally *Bremsstrahlung* does not play a very significant role on the time scale of the spectrum used for elemental analysis. Normally, lower *Bremsstrahlung* backgrounds are also encountered when using UV laser radiation to generate the ablation plasma.

Discriminant analysis

Each spectrum collected using a LIBS instrument is a "finger-print" of the material being analysed and the conditions under which it was collected. Most of the efforts in quantitative LIBS research have been aimed at normalising the spectrum collection conditions and procedures, so that the spectra are sufficiently reproducible for precise quantitative analysis, down to detection sensitivities of a few parts-per-million. In the monitoring process described here, this sophistication is not really required.

Provided that the relative intensity fluctuations related to the reproducibility in the measurement technique itself are smaller then the expected signal variations associated with the element distributions in the sample, the spectra allow for conclusive distinction between specific sample compositions. This is due to the fact that overall irregularities in the spectrum collection procedure can be included in the "finger-print" tolerance of the sample. Thus, an identification rate of close to 100% is possible [25]. The limit of this hypothesis is approached when the sample groups to be identified are very similar, i.e. samples of the same matrix tend to this limit if their trace compositions do not significantly differ between individual samples. However, this does not pose a problem in the case presented here; only differentiation between carious and healthy tissue has to be achieved. This is easy to realise using the pattern recognition algorithm considered here. As a note of caution it should be added that, caries in its early stages might pose a challenge to the recognition algorithm because the difference to healthy tissue may not be very large. However, we have shown for a range of matrices with only subtle compositional differences that our method is still successful [25].

More commonly known as *Discriminant Analysis* in spectroscopy, the aim of any pattern recognition algorithm is to unambiguously determine the identity, or quality of an unknown sample in comparison to a reference database. There are two basic applications for spectroscopic discriminant analysis: (i) material purity / quality determination, and (ii) material identification / screening. In this work we have focused on the latter point, since – to emphasise this again – only unambiguous identification is an issue for monitoring the difference between healthy and carious tissue. It will become evident from the discussion further below that even recognising caries in its early stages of development should be possible in principle.

Material identification and the Mahalanobis Distance method of spectrum matching

When discriminant analysis is used in product-identification, or product-screening mode, the spectrum of the "unknown" sample may be compared against multiple discriminant models. Each model is constructed from the spectra collected from samples representative of various material groups, as defined by the composition of the samples. An indication for the likelihood of the spectrum matching one of these groups emerges from the analysis, and any sample can therefore be classified as a "match", or as a "no-match" (see Figure 2). This identification can be displayed visually on a monitor (e.g. computer screen), or for fast identification can be in the form of a sound signal being activated when e.g. the transition from carious to healthy tooth material was identified. We like to note here that, in principle, only one discriminant model with its related database (training set) would suffice for caries identification. Said data base has to enclose spectra from a wide selection of healthy teeth to provide a statistical means of element concentration scatter; any deviation outside that statistical limit may then be associated with carious tissue. On the other hand, the algorithm has to be "trained" to include only spectral features which are potentially associated with caries since other elemental concentrations may also change, due to other causes (e.g. the presence of a tooth filling). To take into account causes like the one mentioned additional discriminant models might need to be added to unambiguously identify the effect of caries.

Numerous algorithms do exist that can be used to assess the similarity of a measured spectrum with the training

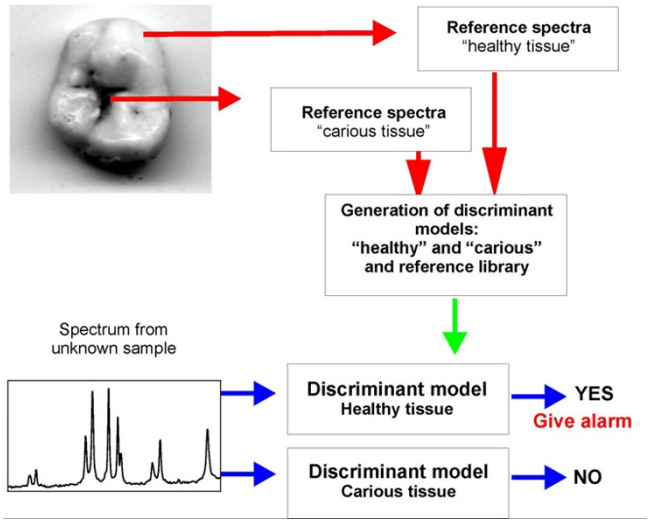

Figure 2
Principle of sample identification / screening applications based on discriminant analysis, here for warning when healthy tooth material is targeted during laser drilling.

set. Here, the description has been restricted to the algorithm of interest, i.e. the so-called *Mahalanobis Distance* Method.

In order to calculate the *Mahalanobis Distance* (M.Dist), *Principle Component Analysis* (PCA) is used. PCA is a typical analytical approach, which normally forms part of any spectral data analysis software package, and thus we abstain here from providing extensive details of such analysis methods and algorithms but only provide a general procedural picture. In PCA / M.Dist analysis training sets of spectra are decomposed into a series of mathematical spectra called *factors* which, when added together, reconstruct the original spectrum. The contribution any factor makes to each spectrum is represented by a *scaling coefficient*, or *score*, which is calculated for all factors identified from the training set. Thus, by knowing the set of factors for the whole training set, the scores will represent the spectra as accurately as the original responses at all wavelengths [25].

Samples under analysis

In this study, we investigated different tooth samples with and without caries – predominantly molar and canine teeth of adults. No special sample treatment was carried out; extracted teeth were just washed out in distilled water and air-dried. One-hundred fifty-nine (159) extracted teeth with different extent of obvious caries (123 molars and 36 canine teeth of adults), which were assessed using visual examination by trained examiners, were used for the results discussed in this publication. The difficult-to-detect early caries lesions, such as in pits or fissures, which are generally non-pigmented or white spot lesions were not included in the study. This was because histopathologic analysis, for correct distinction between carious and healthy tissue in these non-evident cases, was not available at the time of study. Such an extended investigation is now in preparation, in collaboration with two dental practices and a hospital.

Most experiments were carried out *in vitro*. In addition, one test experiment was also conducted *in vivo* on a molar tooth of an adult volunteer. The latter experiment was performed at very low laser irradiance, just above the ablation threshold where the power density is not sufficient to cause noticeable damage to the tooth but nevertheless a luminous plasma is created.

Results and discussion

The Mahalanobis Distance method for matching of LIBS spectra of tooth samples

In order to test this discriminant analysis in the identification of the carious / healthy tissue samples, ten database entries were constructed from the collected spectra to form ten separate *Discriminant Analysis* models, five each from carious and healthy tissues. Six distinct spectral ranges covering a range of matrix and non-matrix elements were used; the relevant spectra are shown in Figure 3. In this way six pairs of "healthy / diseased" identifiers were generated. As pointed our earlier, in principle a single model would probably suffice but having more than one decider naturally improves on the identification accuracy.

For creating the Discriminant Analysis models a list of the training set spectra was simply entered into the *PLS plus/IQ* program attachment to *GRAMS/32* spectral evaluation software package (Galactic Software Ltd.) and linked together with in-house written macro codes for visual (and audio) presentation of the analysis results. The program generated a Discriminant Analysis model for each sample, using the methods outlined in the previous section, against which test spectra were matched. When checking the identity of "unknown" spectra collected from a range of tooth samples, all were either identified as *definite* or *possible* matches to the healthy or diseased tissue discriminant analysis models, even if only one out of the six identifier spectral regions was used.

The major constituent of the tooth's crystalline enamel and dentine matrix structure is hydroxyapatite, $Ca_{10}(PO_4)_6(OH)_2$ whose absolute abundance is distinctly different for healthy dental tissue, and tissue affected by caries. For affected teeth the relative concentrations of the matrix elements *Ca* and *P* decrease severely. On the other hand, non-mineralising (non-matrix) elements, e.g. zinc, and organic materials (the occurrence of the carbon 193

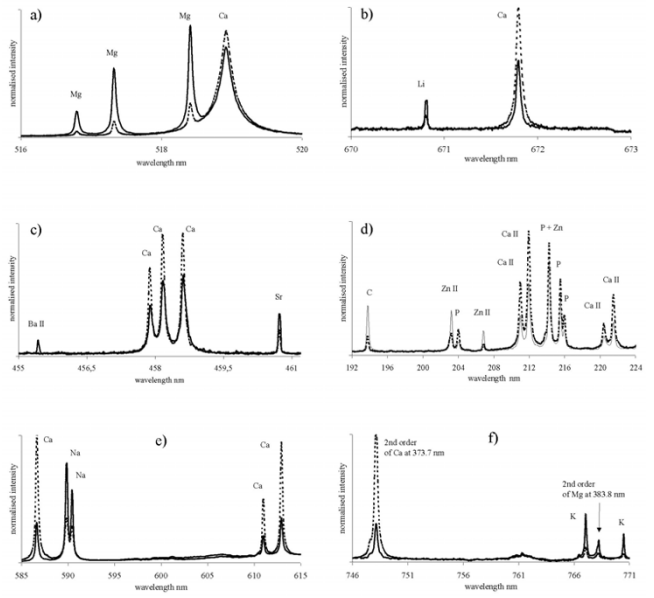

Figure 3
Selected LIBS spectra from an enamel part of the tooth, recorded at a location affected by caries (full line trace) and at a sound, unaffected location (dotted line trace). In the caries-affected section (a) *Ca* diminishes at the expense of *Mg*; (b) *Ca* diminishes at the expense of *Li*; (c) *Ca* diminishes at the expense of *Ba* and *Sr*; (d) *Ca* and *P* diminish at the expense of *Zn* and *C*; (e) *Ca* diminishes at the expense of *Na*; and (f) *Ca* diminishes at the expense of *K* and *Mg*.

nm line is indicative for these) increase strongly; see Figure 3d. A similar indicator for the effect of caries attack is the substantial increase of strontium, *Sr*, and barium, *Ba*, in relation to the matrix element *Ca*; see Figure 3c.

In the Discriminant Analysis models utilised here the important result is the *M.Dist* value. Depending on this, a *pass* (P) – healthy tissue, *possible* (?) – healthy/carious tissue or *fail* (F) – carious tissue – result was returned in the Limits tests, related to particular reference sample groups. Tests carried out on hundreds of spectra recorded from a multitude of different teeth showed conclusive evidence that by using the *M.Dist* values the spectra could be correctly categorised into the two distinct sample groups, namely *sound, healthy tooth area* / *caries-affected tooth area*.

The M.Dist value is effectively a measure of the similarity of an "unknown" spectrum to a group of training spectra. Thus the M.Dist value in Discriminant Analysis models reporting a "*FAIL*" result is normally high, indicating that the spectral contributions from individual elements are very different for e.g. healthy and caries-affected samples. The smaller the M.Dist values for a model giving a "*FAIL*" result the less elemental variations are encountered. On this basis statistical fluctuations in the spectra, caused by inevitable pulse-to-pulse intensity variations, can also be accounted for in the *Prediction Module* by adjusting the M.Dist *PASS*/*FAIL* limits appropriately [25].

As is the case in all Multivariate Quantitative Analysis approaches, careful application is required if the technique is to be applied both correctly and successfully. For example, the limits within which the M.Dist values indicate a match status of *PASS, POSSIBLE* or *FAIL* are frequently defined by default as <2, 2–3, and >3, respectively. For example, Raman spectroscopists often use values greater than these, e.g. <5, 5–15, and >15, respectively. Therefore, these limits always have to be determined prior to a practical application, such as distinguishing between healthy and caries-affected tooth material. The factors, which dictate these limits in LIBS analysis are (i) spectrum reproducibility and (ii) the sample-to-sample homogeneity. By testing the models produced with randomly collected spectra from samples of the material that they represent (carious or sound dental tissue), the range of M.Dist values, which gives a positive identification can be found. If this is not done then the model might incorrectly missidentify materials.

In addition, by carefully adjusting the M.Dist limits, poor reproducibility can in principle be accounted for, provided there are sufficient elemental differences in the samples being sorted, such that clear changes in the spectral responses can be observed. With reference to Figure 3 indeed large differences in the spectral signature of healthy and carious-affected tissue are encountered, and we have shown that in contrast to these obvious cases, subtle differences can also be distinguished (meaning that even the detection of early caries lesions should be feasible). This will be discussed further below, also with reference to the choice of M.Dist limit values.

Finally, we like to note that multivariate analysis is rather unintuitive for the non-expert since a simple graphical representation of the statistical model can not normally be given, as is the case in univariate analysis. In univariate analysis a statistical distribution $f(x)$ is plotted against its variable x, exhibiting a width parameter (confidence limit) $\pm \Delta x$, or $\pm\sigma$. In multivariate analysis, there are many variables x_i, and the function would require a multidimensional plot. For a spectrum with up to a few hundreds of data points (variables) this can not be perceived. The M.Dist value may crudely be interpreted as sort of a confidence limit, similar to the σ in univariate analysis. In order to clarify this point, an example for univariate analysis is given further below. Note that in most analytical cases of well-behaved data multivariate algorithms will provide reduced errors when compared to univariate algorithms.

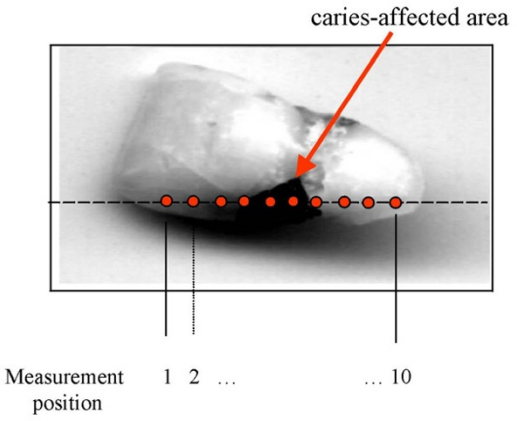

Position	1	2	3	4	5	6	7	8	9	10
Model "healthy"	Y	Y	P	N	N	N	Y	Y	Y	Y
Model "diseased"	N	N	P	Y	Y	Y	P	N	N	N
Continue drilling	*N*	N	*Y*	*Y*	*Y*	*Y*	*N*	*N*	*N*	*N*

Y=yes N=no P=possible

Figure 4
Relationship of M.Dist analysis results across a caries-affected tooth. Measurements were taken at locations spaced at about 1 mm. An "all-clear" indication is given if both models return the correct Y/N combination. The particular data sets were based on spectra according to Figure 3a, containing *Na* and *Ca* lines.

Application of the Mahalanobis Distance method to mapping of carious teeth

From the repeat analysis of the spectra collected from various tooth samples, it could safely be concluded that the Mahalanobis Distance algorithm had the potential of providing a superior tool for matching LIBS spectra and identifying "unknown" sound / carious materials. In this study we achieved close to 100% identification; only one single sample was misinterpreted during our test measurements.

This result is quite remarkable, since the spectra collected in this study were recorded for non-optimised settings. The distal-end of the optical fibre was just mounted at the distance of about 2 mm from the sample for *in vitro* applications, and for the *in vivo* measurements the fibre was simply held by hand while ablating the tooth.

Each spectrum was accumulated for only ten laser-induced plasma events. Fewer laser pulses per spectrum were used at times to speed up the analysis process, but this was at the expense of the spectrum reproducibility, and hence slightly reduced identification probability.

The training spectra utilised in this study were obtained from a range of tooth samples *in vitro* – namely from extracted tooth supplied by dentists.

An example for the strength of the analysis method can be seen in Figure 4. Here an in vitro measurement was carried out on a caries-affected tooth to map the areas of "healthy" and "diseased" tissue. The spectral region used in this specific case was that displayed in Figure 3a (basically including the elements *Mg* and *Ca*). For clarity, only ten measurement positions are indicated, although full raster scans were performed as well. The M.Dist values returned from the analysis according to the two model groups were providing an unequivocal "*PASS*" or "*FAIL*" in the "pure" areas (for a material match the M.Dist value was always smaller than ~1.5, for a mis-match said value normally was >10–100). At the transition boundaries healthy/diseased or diseased/healthy one or the other model test occasionally returned a "*POSSIBLE*" (the ablation area provides material from both "model" species). It should be noted that the example presented here represents only crude, lateral spatial resolution (about 750 µm); in real applications this may become much better with appropriate focussing of the laser radiation. Furthermore, depth resolution is of the order of 1–10 µm, depending on the applied laser pulse energy. Hence, in principle, excellent localised ablation control in three dimensions seems feasible.

As was pointed out further above, univariate analysis of the data may provide a more intuitive insight into the strength of LIBS for the identification of caries. In univariate LIBS analysis, which is the traditional analysis technique, one compares the (amplitude) change of a "trace" element with that of a "matrix" element (where significant changes in composition are encountered one may not have the distinction "trace" versus "matrix"). With reference to Figure 3a, i.e. the spectral region highlighting differences in the relative composition for *Mg* and *Ca* for healthy and carious tissue, one observes a substantial change in the line intensity ratios. In fact, for the two lines *Mg*(518.36 nm) and *Ca*(518.89 nm) the ratio changes from I_{Ca}/I_{Mg} = 4.95 to I_{Ca}/I_{Mg} = 0.90 (healthy-to-caries change). In repeat measurements for a range of healthy tooth samples, when normalising to the strongest peak (*Ca*), the intensity of the other line (*Mg*) varied by about 7%; this is typical in LIBS analysis of matrix materials which are not necessarily completely homogeneous. This statistical fluctuation filters through into the intensity ratio, yielding for the healthy tissue a value of I_{Ca}/I_{Mg} = 4.95 (-0.32/+0.37).

If one were to determine caries in its early stages then evidently the change would not be as dramatic as the one shown in Figure 3 for a far-advanced stage of caries, but

the difference would be subtle. Assuming for the sake of argument that only a change in intensity of 5% of that in Figure 3a were encountered, a ratio I_{Ca}/I_{Mg} = 4.14 (-0.28/ +0.33) would be obtained.

The two values are well outside their respective confidence limits, and thus can easily be distinguished. In principle, one now can set a decision threshold "healthy" / "caries-affected" tissue, according to the I_{Ca}/I_{Mg} ratio. The effectiveness of this approach was demonstrated by moving the ablation area gradually across the caries boundary (laser beam focussed more tightly than during the rest of this study). Only when nearly no overlap with the visually evident caries-affected area ensued did the I_{Ca}/I_{Mg} line ratio come close to the threshold value for "healthy" tissue (actually set to 4.3).

Thus, already with simple univariate (two-point) evaluation a reasonably precise monitoring procedure is at hand. The threshold accuracy is improved even further when applying a multivariate algorithm, as the one used in this study.

We like to stress that the assumption of a 5% change in the "healthy" I_{Ca}/I_{Mg} line ratio value, to reflect early caries, is somewhat arbitrary. A proper histopathologic analysis of various stages of caries would be required to ascertain the appropriate values, and hence the stage at which LIBS analysis could pick up the actual disease state.

Finally, we like to note that similar results to those shown in Figure 4 were obtained in an *in vivo* test measurement, albeit fewer locations on the tooth were probed. Said test was carried out using the "real-time" spectra from a carious-affected molar tooth of an adult volunteer, as mentioned further above. Again we like to emphasise that the laser intensity was kept near threshold levels for plasma generation, in order to prevent damage to the tooth.

Conclusions

In summary, applying the *Mahalanobis Distance* pattern recognition algorithm in discriminant analysis to the evaluation of LIBS spectra recorded from teeth, caries identification was straight-forward. The technique is easy to apply, and the results obtained indicate a near-100% identification rate for materials of both healthy and carious tooth sections.

If correctly applied, the combination of LIBS and discriminant analysis could provide a useful tool for *in vivo* / *in vitro* caries identification during the drilling process when a luminous plasma is created by short laser pulses. Since the generation of a (luminous) plasma is inherent to the laser ablation process, any of the actual laser sources currently used in dental treatment tests, not only the Nd:YAG laser utilised in this study, should be suitable for the implementation of the proposed technique. Positive / negative identification could be signalled e.g. by a short sound when the transition from caries to healthy tooth material is identified by the pattern recognition algorithm. This would allow the dentist to follow normal drilling routines while obtaining automatic, real-time information about the composition of the sample area and the status of ablation.

Finally, we would like to stress that our study should be seen as a proof of principle rather than a fully-developed analytical method. For this repeat measurements with actual dental laser system need to be carried out, and in particular more extensive *in vivo* studies are required. Furthermore, proper histopathologic analysis, for correct distinction between carious and healthy tissue in non-evident cases, has to be performed to provide absolute calibration standards.

Competing Interests

None declared

Acknowledgements

O Samek gratefully acknowledges the financial support for this study through Grant CEZ:J22/98:262100002.

References

1. Murray JJ: **The prevention of Dental Disease.** *Oxford University Press, Oxford* 1990
2. Niemz MH: **Laser-tissue interactions.** *Springer Verlag, Berlin* 1996
3. Takamori K, Hokari N, Okumura Y, Watanabe S: **Detection of oclusal caries under sealant by use of a laser fluorescence system.** *J Clin Laser Med Surgery* 2001, **19**:267-271
4. Stookey GK, Gonzales-Cabezas C: **Emerging methods of caries diagnosis.** *J Dent Educ* 2001, **65**:1001-1006
5. Schneiderman A, Elbaum M, Schultz T, Keem S, Greenebaum M, Driller J: **Assessment of dental caries with Digital Imaging Fibre-Optics Transillumination (DIFOTI): in vitro study.** *Caries Res* 1997, **31**:103-110
6. Nair MK, Tyndall DA, Ludlow JB, May K: **Tuned aperture computed tomography and detection of recurrent caries.** *Caries Res* 1998, **32**:23-30
7. Abreu M, Tyndall DA, Ludlow JB, Nortje CJ: **The effect of the number of iterative restorations on tuned aperture computed tomography for approximal caries detection.** *Dentomaxillofac Radiol* 2001, **30**:325-329
8. Wenzel A: **Digital radiography and caries diagnosis.** *Dentomaxillofac Radiol* 1998, **27**:3-11
9. Zero DT: **Applications of clinical models in remineralization research.** *J Clin Dent* 1999, **10**:74-85
10. McIntyre JM, Featherstone JDB, Fu J: **Studies of dental root surface caries. 2: The role of cementum in root surface caries.** *Australian Dent J* 2000, **45**:97-102
11. Kruger J, Kautek W, Newesely H: **Femtosecond-pulse laser ablation of dental hydroxyapatite and single-crystalline fluoroapatite.** *Appl. Phys. A* 1999, **69**:S403-407
12. Kohns P, Zhou P, Stormann R: **Effective laser ablation of enamel and dentine without thermal side effects.** *J. Laser Appl* 1997, **9**:171-174
13. Hibst R: **Applications of lasers in dentistry – a survey.** *LaserOpto* 2000, **32**:46-52
14. Fried D, Zuerlein M, Featherstone JDB, Seka W, Duhn C, McCormack SM: **IR laser ablation of dental enamel: mechanistic dependence on the primary absorber.** *Applied Surface Science* 1998, **127-129**:852-856

15. Altshuler GB, Belikov AV, Sinelnik YA: **A laser-abrasive method for the cutting of enamel and dentine.** *Laser Surg Med* 2001, **28**:435-444
16. Fried D, Ragadio J, Champion A: **Residual heat deposition in dental enamel during IR laser ablation at 2.79, 2.94, 9.6 and 10.6 μm.** *Laser Surg Med* 2001, **29**:221-229
17. Eguro T, Maeda T, Tanabe M, Otsuki M, Tanaka H: **Adhesion of composite resins to enamel irradiated by the Er:YAG laser: application of the ultrasonic scaler on irradiated surface.** *Laser Surg Med* 2001, **28**:365-370
18. Jeffries T: **Quintupled YAG probes 200-year-old teeth to uncover ancient diet details.** *Opto Laser Europe* 2001, **issue 84(May 2001)**:15
19. Majidi V, Joseph MR: **Spectroscopic Applications of Laser-Induced Plasmas.** *Critical Reviews in Analytical Chemistry* 1992, **23**:143-162
20. Radziemski LJ: **Review of Selected Analytical Applications of Laser Plasmas and Laser Ablation 1987–1994.** *Microchemical Journal* 1994, **50**:218-234
21. Samek O, Liška M, Kaiser J, Beddows DCS, Telle HH, Kukhlevsky S: **Clinical application of laser-induced breakdown spectroscopy to the analysis of teeth and dental materials.** *J. Clinical Laser Medicine & Surgery* 2000, **18**:281-289
22. Beddows DCS, Kondo H, Morris GW, Telle HH: **Remote laser-induced breakdown spectroscopy using a novel single-fibre arrangement.** *CLEO/Europe – EQEC '98, Glasgow 1998: Technical Digest* 237
23. Samek O, Beddows DCS, Kaiser J, Kukhlevsky S, Liška M, Telle HH, Young J: **The application of laser induced breakdown spectroscopy to in situ analysis of liquid samples.** *Optical Engineering* 2000, **39**:2248-2262
24. Amador-Hernandez J, Fernandez-Romero JM, Luque de Castro MD: **In-depth characterization of screen-printed electrodes by laser-induced breakdown spectroscopy and pattern recognition.** *Surf. Interface Anal* 2001, **31**:313-320
25. Samek O, Krzyzanek V, Beddows DCS, Telle HH, Kaiser J, Liška M: **Material identification using laser spectroscopy and pattern recognition algorithms.** *Lecture Notes in Computer Science* 2001, **2124**:443-450